ACS APPLIED MATERIALS & INTERFACES

RESEARCH ARTICLE

www.acsami.org

Water-Processable Polyaniline with Covalently Bonded Single-Walled Carbon Nanotubes: Enhanced Electrochromic Properties and Impedance Analysis

Shanxin Xiong,[†] Jia Wei,[‡] Pengtao Jia,[†] Liping Yang,[†] Jan Ma,[†,‡] and Xuehong Lu*[,†,‡]

[†]Temasek Laboratories, Nanyang Technological University, 50 Nanyang Drive, Singapore 637553

[‡]School of Materials Science and Engineering, Nanyang Technological University, 50 Nanyang Avenue, Singapore 639798

Supporting Information

ABSTRACT: Hybrid electrochromic materials were readily synthesized via copolymerization of aniline with *p*-phenylenediamine-functionalized single-walled carbon nanotubes (SWCNTs) in the presence of poly(styrene sulfonate) (PSS) dopant in an aqueous medium. Polyaniline (PANI)-grafted SWCNTs are formed, and they are uniformly dispersed in the PANI/PSS matrix. Impedance analysis shows that the charge-transfer resistances of the hybrids at all states are reduced drastically with increasing SWCNT loading. With 0.8 wt % SWCNTs, the charge-transfer resistances of the hybrid at +1.5 and −1.5 V are only about 20% and 12% of those of PANI/PSS, respectively, which is due to the greatly increased redox reactivity given by the enhanced electron transport in the hybrid and further doping function of the SWCNTs. The remarkable increase in redox reactivity leads to much enhanced electrochromic contrast from 0.34 for PANI to 0.47 for PANI-SWCNT-0.8%.

KEYWORDS: polyaniline, carbon nanotubes (CNT), covalent bonding, electrochromism

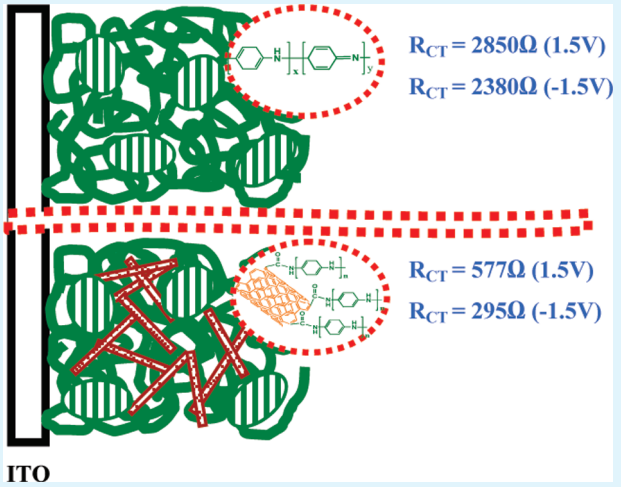

INTRODUCTION

Since carbon nanotubes (CNTs) were reported by Iijima in 1991, they have been extensively studied and widely applied in numerous fields[1] because of their unique one-dimensional nanostructure and outstanding mechanical and electrical properties. In particular, their excellent electron-transport property and high electrochemical stability make them ideal candidates for fabrication of electronic, optoelectronic, and electrochemical devices in conjunction with conjugated polymers. The strong $\pi-\pi$ interactions between CNTs and conjugated polymers often lead to synergistic effects in improving performances of the devices such as organic light emitting diodes,[2] photovoltaics,[3] supercapacitors,[4] and sensors.[5]

The preparation, structures, morphologies, and properties of conjugated polymer/CNT nanocomposites have been widely studied. Smith et al. prepared polyaniline (PANI)/multiwalled carbon nanotubes (MWCNTs) nanocomposites through in situ polymerization of aniline in the presence of acid-modified MWCNTs and studied the interactions between PANI and the MWCNTs. They found that the MWCNTs can act as dopants to interact with both N−H groups and quinoid units on the PANI backbone, which increases the degree of electron delocalization and hence leads to enhanced electrical conductivity of the material.[6] Li et al. reported in situ polymerization of aniline in the presence of acid-modified MWCNTs for anodic materials in high-power microbial fuel cells. It was found that the composite anode containing 20 wt % MWCNTs gave the best discharge performance as the interfacial charge-transfer resistance declines greatly with increasing MWCNT content in the composite films,[7] facilitating the electrochemical reactions on the electrode. Recently, Deepa et al. reported poly(3,4-ethylenedioxythiophene) (PEDOT)/MWCNT nanocomposites prepared via electrochemical polymerization of the monomer in the presence of MWCNTs for electrochromic application.[8] They found that the high electrical conductivity and doping effect of the acid-modified MWCNTs led to improvements in electrochemical activity and coloration efficiency of PEDOT.

PANI is one of the most widely used anodically coloring electrochromic polymers owing to its ease of preparation and good environment stability. It exhibits multicolor electrochromism

Received: November 18, 2010
Accepted: January 31, 2011
Published: February 21, 2011

in the visible region as well as electrochromism in the infrared region.[9] Furthermore, when doped with poly(styrene sulfonate) (PSS), PANI can be well dispersed in aqueous media, and the polymeric dopants render the doped PANI higher electrochemical stability as the large anions can be more or less confined in PANI during the redox switching, which protects the bipolaron from nucleophilic attack by either hydroxyl ions or water molecules.[10] However, in comparison with small-molecule dopants, such as dodecylbenzene sulfonic acid, PSS dopant causes lower optical contrast and slower kinetics of the PANI-based electrochromic devices owing to the excess amount of PSS units in the system and low mobility of PSS anions.[11] In this work, in order to make more PANI units redox active to boost the electrochromic contrast, we covalently grafted PANI chains to carbon nanotubes to improve the electron transport in PANI/PSS. Instead of MWCNTs, single-walled carbon nanotubes (SWCNTs) were used in this work as they possess larger surface area and higher electric conductivity and hence may bring about greater improvement in electrochromic performance. The good dispersion of the SWCNTs in PANI/PSS achieved through covalent bonding would ensure the large interfacial area, leading to substantial interactions between PANI and the SWCNTs. Herein, we demonstrate that, with the PANI-grafted SWCNTs, this new class of water-processable hybrid materials exhibits significantly enhanced electrochromic contrast and switching kinetics. The underlying mechanism for the enhancements is illustrated with impedance analysis.

EXPERIMENTAL SECTION

Functionalization of SWCNTs. All chemicals were purchased from Sigma-Aldrich and used as received unless specified otherwise. SWCNTs were obtained from Carbon Solutions, Inc. The SWCNTs were first heat treated at 400 °C in air and oxidized with concentrated nitric acid and sulfuric acid to yield carboxylic acid-functionalized SWCNT (SWCNT-COOH).[12] The SWCNT-COOH was then reacted with thionyl chloride and *p*-phenylenediamine (PPD) according to the procedure reported by Philip et al.,[13] except that the pyridine was replaced by triethylamine and the solvent was changed to toluene. The resultant PPD-functionalized SWCNT (SWCNT-PPD) was stored in *N*,*N*-dimethyl formamide (DMF).

Preparation of PANI-SWCNT Hybrids. A series of PANI-SWCNT samples were synthesized through copolymerization of SWCNT-PPD with aniline in an aqueous solution with PSS (M_w = 75 000) as the dopant. First, a specified amount (5.54, 11.08, and 22.16 mg, respectively) of SWCNT-PPD was dispersed in a solution consisting of 10.22 g of 18 wt % PSS aqueous solution, 0.93 g of aniline, and 100 g of water with the aid of ultrasonication. The solution was stirred in an ice−water bath for 30 min. Ammonium peroxydisulfate (2.28 g) in 13 mL of water was then dropped into the solution in three separate doses in 30 min. The reaction was carried out for 24 h in a stirred ice−water bath, producing PANI-SWCNT aqueous solutions. The three samples with feed SWCNT-PPD loadings of 5.54, 11.08, and 22.16 mg are denoted as PANI-SWCNT-0.2%, PANI-SWCNT-0.4%, and PANI-SWCNT-0.8%, respectively, in this paper. To confirm the grafting reaction, PANI-grafted SWCNTs were obtained by removing most ungrafted PANI through repeatedly washing PANI-SWCNT-0.8% with water, and the sample is denoted as PANI-*g*-SWCNT. PANI/PSS was also synthesized as a reference material, which was prepared using the same procedure as that used for the PANI-SWCNT samples but without the addition of SWCNT-PPD.

Fabrication of Electrochromic Devices. Aqueous solutions of the PANI/PSS and PANI-SWCNT hybrids with different SWCNT contents were spin-coated onto 3 cm × 3 cm indium tin oxide (ITO)-coated polyethylene terephthalate (PET) substrates (100 Ω/□). The thin film thickness was measured using an Alpha-Step 500 profilometer. For easy comparison, the thicknesses of all electrochromic layers were controlled carefully to be 170 nm through adjusting the spin-coating speed. The electrochromic devices with sandwiched structure of PET/ITO/electrochromic layer/polymer gel electrolyte/ITO/PET were fabricated according to the methods described in our previous publication.[14] The polymer gel electrolyte used was a mixture of 0.512 g of $LiClO_4$, 2.8 g of PMMA, 8 g of propylene carbonate, and 28 g of acetonitrile.

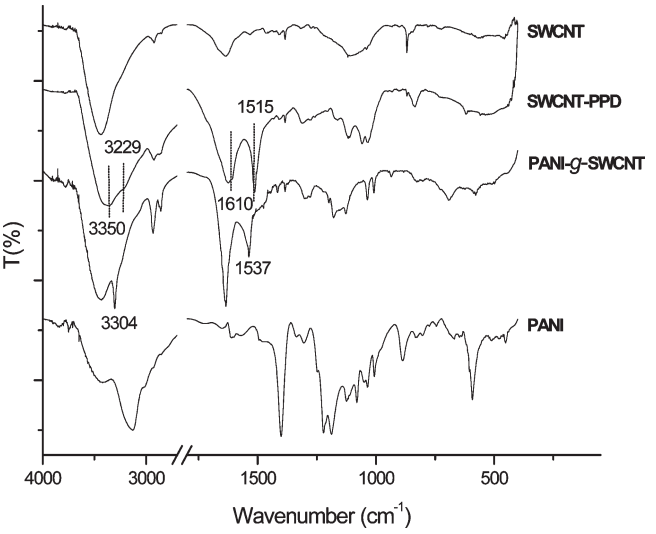

Figure 1. FTIR spectra of the SWCNT, SWCNT-PPD, PANI-*g*-SWCNT and PANI.

Characterization. Fourier transform infrared (FTIR) spectra of the materials were obtained on a Perkin-Elmer GX spectrometer using KBr method. Thermo-gravimetric analysis (TGA) was conducted using a TA Q500 TGA at a heating rate of 10 °C/min from 40 to 800 °C in N_2. Prior to the heating, the samples were isothermal at 120 °C for 1 h to remove a trace amount of water. The field-emission scanning electron microscopic (FE-SEM) images of the materials were obtained on a JEOL 7600F SEM. Before observation, the PANI-SWCNT-0.8% film was etched by water to partially remove the ungrafted PANI and PSS. The transmission electron microscopic (TEM) images of PANI-*g*-SWCNT were obtained on a JEM-2010 TEM. The cyclic voltammetry (CV) experiments were carried out using Pt (99.99%) and Ag wires (99.9%) as counter and pseudoreference electrodes, respectively, in a 0.1 M $LiClO_4$/acetonitrile electrolyte solution. The pseudoreference silver wire was calibrated vs Fc/Fc^+ by dissolving ferrocene in the electrolyte solution and determining the $E_{1/2}$ of the Fc/Fc^+ against the silver wire. The working electrode was obtained by spin-coating an electrochromic layer on PET/ITO sheet. The UV−vis spectra of the dilute solutions in water were obtained using a SHIMADZU 2501 spectrometer. In situ spectroelectrochemical properties of the devices were recorded using an Autolab PGSTAT30 potentiostat with the UV−vis spectrometer (SHIMADZU 2501). The impedance of the films was determined over the frequency range of 10^6-10^{-2} Hz with signal amplitude of 10 mV using Autolab PGSTAT30 potentiostat with the same three-electrode electrochemical cell as that used in CV testing. The potentials were applied vs open circuit potential (OCP) of cell.

RESULTS AND DISCUSSION

Synthesis and Morphology of the PANI-SWCNT Hybrids. The synthesis scheme for the hybrids is shown in Scheme 1. The

Scheme 1. Synthesis Route for the PANI-*g*-SWCNT

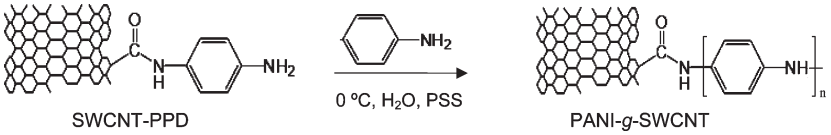

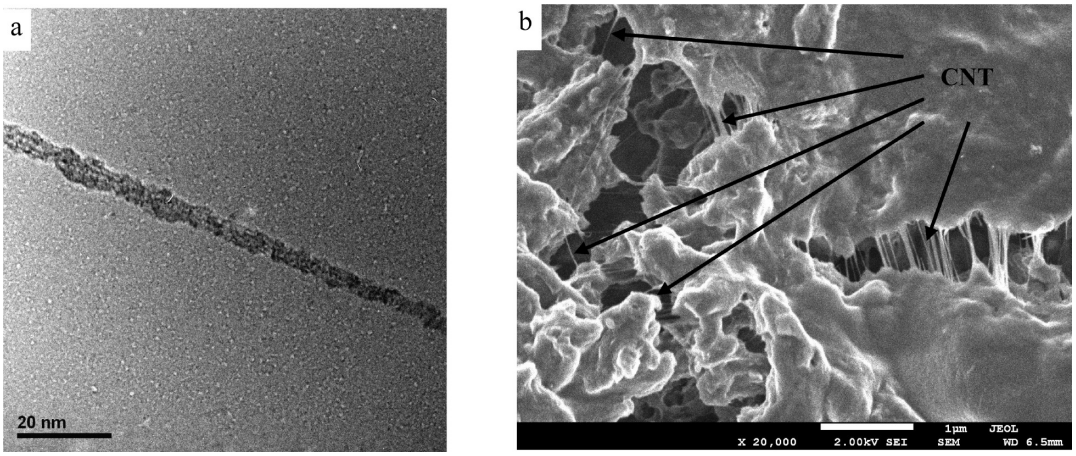

Figure 2. (a) TEM image of PANI-*g*-SWCNT, showing that the SWCNTs are enwrapped by PANI, and (b) FE-SEM image of partially etched PANI-SWCNT-0.8% film, showing that the SWCNTs are dispersed uniformly in PANI matrix in forms of both single tubes and bundles.

functional groups on the SWCNTs were characterized using FTIR (Figure 1). In the SWCNT-PPD spectrum, the presence of intensive bands at 1515 cm^{-1} (benzene ring stretching) and 1610 cm^{-1} (amide II band) and weak doublets at 3229 and 3350 cm^{-1} (N−H stretching of primary amine) confirms the successful grafting of aniline groups on the SWCNTs.[13,15] The TGA result shows that the weight loss of SWCNT-PPD from 150 to 450 °C is about 23%, which can be viewed as the rough content of the organic groups (cf. Supporting Information, Figure S1). The SWCNT-PPD suspensions in DMF and water are fairly stable, which makes grafting SWCNTs with PANI in aqueous system possible. In the presence of PSS dopant molecules, the aniline groups on SWCNT-PPD can copolymerize with aniline monomer, forming PANI-*g*-SWCNT in complex with PSS. Since the contents of SWCNT-PPD are very low, the as-polymerized samples (PANI-SWCNT) contain both PANI-*g*-SWCNT and ungrafted PANI chains. The three PANI-SWCNT samples with different SWCNT contents show almost same FTIR spectra (cf. Supporting Information, Figure S2). The characteristic bands of PANI and PSS appear at 1490 cm^{-1} (stretching mode of C−C in benzenoid unit), 1608 cm^{-1} (stretching mode of C−C in quinoid unit), 1035 cm^{-1} ($-SO_3H$), and 1122 cm^{-1} ($-SO_2-$stretching),[16] respectively. To confirm that PANI chains had been grafted onto the SWCNTs, most ungrafted PANI chains and PSS were washed out with water. The FTIR spectrum of PANI-*g*-SWCNT is distinctly different from that of SWCNT-PPD and PANI/PSS (Figure 1). The doublets (N−H stretching of primary amine) disappear, and a sharp N−H stretching band appears at 3304 cm^{-1}, confirming that the aniline group on SWCNT-PPD has copolymerized with aniline monomer. In addition, the benzene stretching band at 1515 cm^{-1} for SWCNT-PPD is shifted to 1537 cm^{-1} for PANI-*g*-SWCNT, owing to the rigid conjugated structure of the grafted PANI chains.

After copolymerization with aniline, the SWCNTs are enwrapped by PANI chains. The TEM study shows that, after washing out free PANI chains and PSS, some SWCNTs are enwrapped by PANI as single tube (Figure 2a), which further confirms that PANI has been tethered onto SWCNTs successfully. To study the dispersion state of the PANI-g-SWCNT in the spin-coated films, FE-SEM images were taken from partially etched PANI-SWCNT-0.8% film (Figure 2b). It shows that, in SWCNT rich regions, some SWCNTs may be in bundle form. Nevertheless, the SWCNTs can be observed in almost all the extensively etched regions, indicating a fairly uniform dispersion of the SWCNTs in the PANI matrix. The SWCNTs covalently incorporated in the PANI/PSS matrix can enhance the electron-transport property of the material significantly, especially when the PANI is at its low conductive states, and hence will influence electrochemical and electrochromic properties of the PANI, as will be shown later.

Electrochemical and Electrochromic Properties of the Hybrids. The CV curves of the PANI/PSS and PANI-SWCNT hybrid films obtained from the sweeps between −0.7 and +1.5 V show that all samples exhibit two oxidation peaks and two reduction peaks (Figure 3a), which can be assigned to the leucoemeraldine salt (LES) to emeraldine salt (ES) and ES to pernigraniline salt (PNS) transitions, respectively, and the corresponding reverse transitions. The intensities of the oxidation and reduction peaks all increase significantly with increasing SWCNT content in the hybrids. It is striking to see that the peak current density of PANI-SWCNT-0.8% is two times higher than that of the PANI/PSS. Accompanied by this, the charge density is almost doubled, i.e., increased drastically from 3.78 mC/cm^2 (injection) and 3.67 mC/cm^2 (extraction) for the PANI/PSS to 7.00 mC/cm^2 (injection) and 8.01 mC/cm^2 (extraction) for PANI-SWCNT-0.8% (Figure 3b). The higher charge densities of the hybrids indicate that they have larger charge-storage

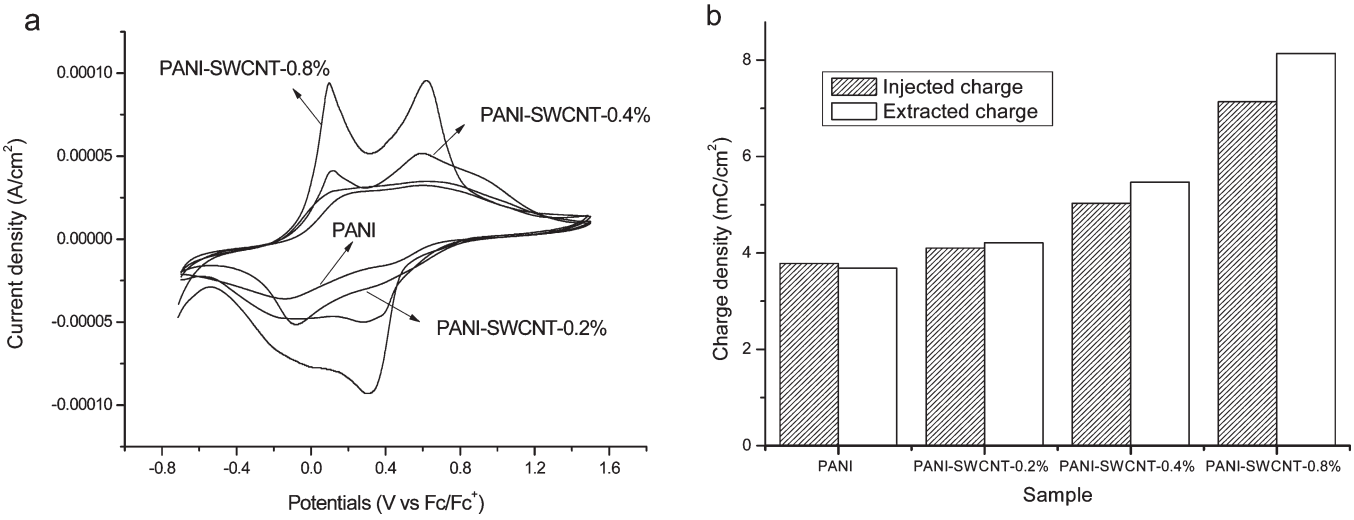

Figure 3. (a) Cyclic voltammograms of the PANI, PANI-SWCNT-0.2%, PANI-SWCNT-0.4%. and PANI-SWCNT-0.8%. (b) The plots of charge densities as functions of SWCNT content.

Table 1. Electrochromic Properties of the Neat PANI and PANI-SWCNT Hybrids

	PANI	PANI-SWCNT-0.2%	PANI-SWCNT-0.4%	PANI-SWCNT-0.8%
ABS λ_{max} (nm)[a]	778	775	772	768
contrast (ΔA) at λ_{max} (nm)[b]	0.34/680	0.36/660	0.43/655	0.47/630
coloration efficiency (cm^2/C)	105	114	159	168

[a] The wavelength at maximum absorbance (λ_{max}) measured in dilute solutions without applying external potential. [b] The λ_{max} of the single-active-layer devices was measured at +2.0 V. The absorbance change of the devices at λ_{max} was determined by switching from −2.8 to +2.0 V.

capacities, which may be attributed to the improved redox activity of the PANI matrix as well as the large surface area of the SWCNTs and open morphology of the hybrids caused by the well dispersed SWCNTs.[17]

In addition to the increased peak current densities and charge densities, peak shifts can also be observed. In particular, the first oxidation peak is shifted from 0.22 V for PANI/PSS to 0.10 V for PANI-SWCNT-0.8%. This may be attributed to the conductive function of the SWCNTs that lowers down the voltage drop across the film during the switching and the further doping of the SWCNTs that renders the PANI a slightly higher doping level.[18] The further doping is evidenced by the blue shift of the π-polaron peak of the PANI at neutral state with increasing SWCNT content, as listed in Table 1 (cf. Supporting Information, Figure S3). The reduction of oxidation potentials of PANI-SWCNT makes the oxidation process easier and hence benefits the Li^+ extraction at the oxidation state, which explains why the increase in extraction charge density is slightly larger than that in injection charge density with increasing SWCNT content.

Figure 4 shows the in situ spectroelectrochemical properties of the devices with the PANI/PSS and PANI-SWCNT hybrids as the electrochromic layer, respectively. Under negative potentials, the absorption peaks are red-shifted to long-wavelength direction in the dedoping process of PANI, and the color of the devices are greenish yellow. Under positive potentials, the peaks are blue-shifted to short-wavelength direction in the doping process of PANI, and the devices become sky blue. The typical photographs of the device at these two color states are shown in Supporting Information, Figure S4. When switching from −2.0 to +2.0 V, the PANI/PSS exhibits a total change in absorbance (ΔA) of 0.34 at the wavelength at the maximum absorbance (λ_{max}) of 680 nm. With increasing SWCNT content, the optical contrast, i.e., the ΔA at λ_{max} increases. PANI-SWCNT-0.8% shows the highest contrast of 0.47 at its λ_{max} of 630 nm. In comparison with the neat PANI, PANI-SWCNT-0.8% exhibits nearly 40% contrast enhancement and 50 nm blue shift. The other PANI-SWCNT hybrids also show improved contrast and peak shift of different degrees (cf. Supporting Information, Figure S5), as listed in Table 1. The enhanced contrast and blue shift are ascribed to the improved electron transport in the hybrids and further doping of the SWCNTs. The well-dispersed PANI-*g*-SWCNT could lower down the charge-transfer resistance, reduce the voltage loss across the electrochromic layer, and make the potential more evenly applied; thus, more PANI units are electrochemically active. The further doping function of the SWCNTs facilitates the oxidation of PANI, resulting in higher contrasts at the same effective potentials. In other words, in comparison with the PANI-based device, the PANI-SWCNT-based devices can achieve the same contrast at lower potentials, reducing the possibility of overoxidation of PANI during device switching and, hence, benefiting the long-term stability of the device. Besides the enhancement in contrast, the incorporation of SWCNT into PANI also leads to improved coloration efficiency (CE), which similar to the effect of MWCNT reported by Bhandari et al.[8] The CE values of PANI and PANI-SWCNT-based devices are listed in Table 1.

The improved electron transport and further doping function also benefit the switching kinetics of the devices (Figure 4c). In comparison with small-molecule dopants, polymeric acid-doped PANI exhibits much slower switching kinetics, owing to the low mobility of the macromolecular anions during the switching process. In this study, an aqueous system with PSS

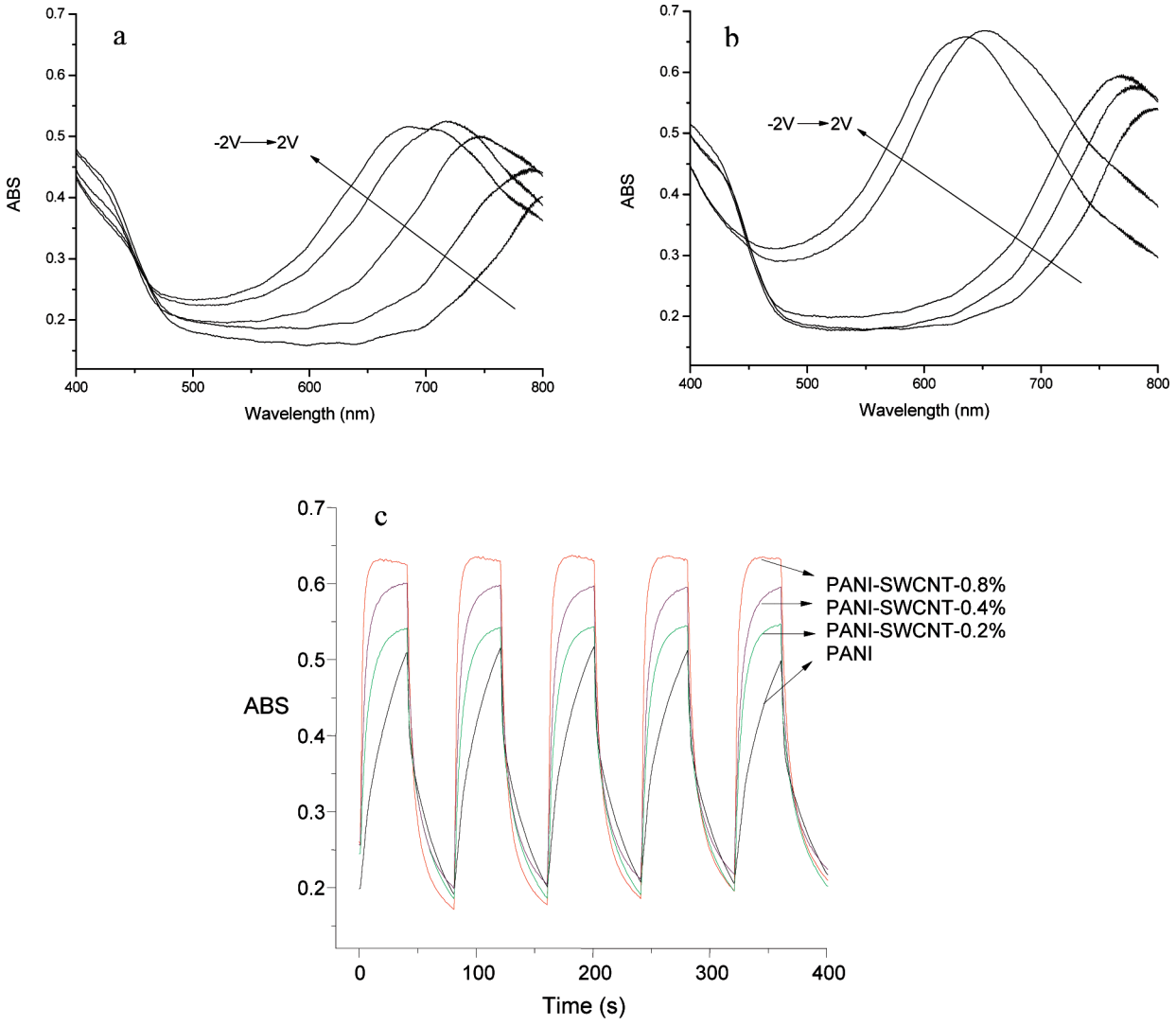

Figure 4. Absorption spectra of the electrochromic devices with (a) PANI and (b) PANI-SWCNT-0.8% as the electrochromic layer, respectively, at potentials of −2, −1, 0, 1, and 2 V in the visible range. (c) Optical absorbance at λ_{max} for the devices with PANI, PANI-SWCNT-0.2%, PANI-SWCNT-0.4%, and PANI-SWCNT-0.8% as the electrochromic layers, respectively, under the step potential oscillating between +2.0 and −2.8 V with a 40 s interval.

macromolecular dopant is utilized to realize a more environmental friendly system. It can be seen that the switching curve of the neat PANI-based device has fairly flat slopes at both its coloration and bleaching states. With increasing SWCNT content, both the coloration and bleaching curves become steeper, indicating the faster switching kinetics of the devices. Owing to the relative low electric conductivity of PANI at its bleaching state, the enhancement in switching kinetics of the bleaching process is not as significant as that of coloration process. Also, with 0.8% SWCNT, the initial part of the coloration curve is much steeper than that of the bleaching curve, as the hybrid can be oxidized more easily than the neat PANI, owing to the further doping of the SWCNTs.[18]

Impedance Analysis. To verify the mechanism for the significantly improved optical contrast and switching kinetics brought by the covalently bonded SWCNTs, AC impedance studies were carried out to analyze the electron and ion movements across the electrode/electrolyte interfaces and assess the redox activities of the materials at various states. With negative or positive potentials applied, semicircles appear in the Nyqvist plots in the midrange frequencies (cf. Supporting Information Figure S6), signifying charge-transfer processes. The charge-transfer resistances, R_{CT}, determined from the diameters of the semicircles in the Nyqvist plots are plotted in Figure 5 as functions of the potential applied. For both the PANI/PSS and PANI-SWCNT hybrids, with an increase in the positive potentials or a decrease in the negative potentials, the R_{CT} decreases. At low potentials, the systems with high charge-transfer resistance are electrochemically inactive, whereas at higher potentials, doping−dedoping processes that involve injection/removal of electrons in the polymer film balanced by counterions diffusion from/to the electrolyte will activate the electrochemical reactions, as well as reduce the charge-transfer resistance.[19] Under negative potentials, Li^+ and H^+ ions can be easily injected into the films owing the PSS anions confined in the films, resulting in lower charge-transfer resistance than that at positive potentials. However, this does not mean that the bleaching is easier than the coloring of the PANI/PSS film as the electron-transport property of the PANI/PSS is poor at the reduced state. With increasing the SWCNT loading, the charge-transfer resistances of the hybrid

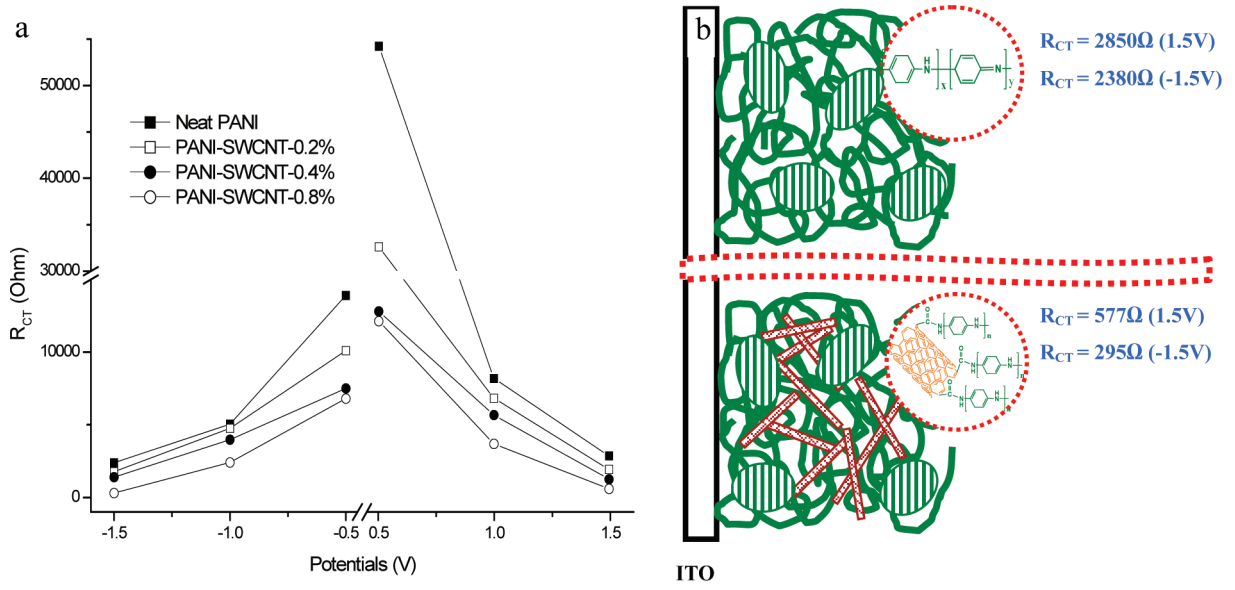

Figure 5. (a) Charge-transfer resistance as functions of the applied potential and (b) a scheme showing structures of the neat PANI and PANI-SWCNT films.

films are decreased sharply, owing to the improved electron transport in the hybrids brought by the covalently bonded SWCNTs, especially when the matrix is at semiconductive states (0.5 V) since the well dispersed PANI-*g*-SWCNT may greatly reduce tunneling length between conductive domains, which is normally embraced in amorphous regions with poor conductivity (Figure 5b).[20] Under the highest positive or negative potentials, which correspond to fully doped and dedoped states of PANI (insulated states), the well-dispersed SWCNTs and high potentials improve the electrochemical activity of PANI very significantly. Under +1.5 V potential, the R_{CT} of the PANI/PSS is 2850 Ω, whereas with the introduction of SWCNT, the R_{CT} is declined to 1920, 1220, and 577 Ω for 0.2, 0.4, and 0.8 wt % feed loading of SWCNTs, respectively. Similarly, under −1.5 V, the R_{CT} is declined from 2380 to 1770, 1390, and 295 Ω, respectively. The much reduced charge-transfer resistances at high potentials are due to the accelerated redox reactions caused by the enhanced electron transport.

CONCLUSIONS

Covalently bonded PANI-SWCNT hybrids were readily synthesized via copolymerization of aniline with SWCNT-PPD in aqueous solutions containing PSS. The presence of PANI-grafted PANI leads to the well dispersion of the SWCNTs in the PANI/PSS matrix and facilitates the electron transport and interaction between the SWCNTs and PANI. The enhanced electron transport in the electrochromic layer greatly improves its redox reactivity, especially when PANI is switched to its low conductive states, as evidenced by the significantly reduced charge-transfer resistances. The substantial interaction between the SWCNTs and PANI gives a significant further doping effect, reducing the oxidation potential of the PANI. These render the corresponding electrochromic devices much improved optical contrast and switching kinetics. Comparing with the neat PANI, the PANI-SWCNT hybrids would exhibit the same contrast at much lower potentials, which may also benefit the lifetime of the devices.

ASSOCIATED CONTENT

Supporting Information. TGA curves, FTIR spectra, UV−vis spectra, photographs of the device at different color states, absorption spectra of the PANI and PANI-SWCNT hybrid-based devices and Nyqvist plots of PANI-SWCNT films. This material is available free of charge via the Internet at http://pubs.acs.org.

REFERENCES

(1) (a) Pichler, T.; Knupfer, M.; Golden, M. S.; Fink, J.; Rinzler, A.; Smalley, R. E. *Phys. Rev. Lett.* **1998**, *80*, 4729. (b) Yosida, Y.; Oguro, I. *J. Appl. Phys.* **1999**, *86*, 999. (c) Zahab, A.; Spina, L.; Poncharal, P.; Marlière, C. *Phys. Rev. B* **2000**, *62*, 10000. (d) Jouguelet, E.; Mathis, C.; Petit, P. *Chem. Phys. Lett.* **2000**, *318*, 561. (e) Hong, K.; Yang, C.; Kim, S. H.; Jang, J.; Nam, S.; Park, C. E. *ACS Appl. Mater. Interfaces* **2009**, *1*, 2332.

(2) (a) Curran, S. A.; Ajayan, P. M.; Blau, W. J.; Carroll, D. L.; Coleman, J. N.; Dalton, A. B.; Davey, A. P.; Drury, A.; McCarthy, B.; Maier, S.; Stevens, A. *Adv. Mater.* **1998**, *10*, 1091. (b) Nurmawati, M. H.; Renu, R.; Ajikumar, P. K.; Sindhu, S.; Cheong, F. C.; Sow, C. H.; Valiyaveettil, S. *Adv. Funct. Mater.* **2006**, *16*, 2340.

(3) Ago, H.; Petritsch, K.; Shaffer, M. S. P.; Windle, A. H.; Friend, R. H. *Adv. Mater.* **1999**, *11*, 1281.

(4) Chen, G. Z.; Shaffer, M. S. P.; Coleby, D.; Dixon, G.; Zhou, W.; Fray, D. J.; Windle, A. H. *Adv. Mater.* **2000**, *12*, 522.

(5) (a) An, K. H.; Jeong, S. Y.; Hwang, H. R.; Lee, Y. H. *Adv. Mater.* **2004**, *16*, 1005. (b) Kaempgen, M.; Roth, S. *J. Electroanal. Chem.* **2006**, *586*, 72.

(6) Zengin, H.; Zhou, W.; Jin, J.; Czerw, R.; Smith, D. W., Jr.; Echegoyen, L.; Carroll, D. L.; Foulger, S. H.; Ballato, J. *Adv. Mater.* **2002**, *14*, 1480.

(7) Qiao, Y.; Li, C. M.; Bao, S.-J.; Bao, Q.-L. *J. Power Sources* **2007**, *170*, 79.

(8) Bhandari, S.; Deepa, M.; Srivastava, A. K.; Lal, C.; Kant, R. *Macromol. Rapid Commun.* **2008**, *29*, 1959.

(9) Topart, P.; Hourquebie, P. *Thin Solid Films* **1999**, *352*, 243.

(10) Lippe, J.; Holze, R. *J. Electroanal. Chem.* **1992**, *339*, 411.

(11) Xiong, S.; Jia, P.; Mya, K. Y.; Ma, J.; Boey, F.; Lu, X. *Electrochim. Acta* **2008**, *53*, 3523.

(12) Kumar, N. A.; Kim, S. H.; Kim, J. S.; Kim, J. T.; Jeong, Y. T. *Surf. Rev. Lett.* **2009**, *16*, 487.
(13) Philip, B.; Xie, J.; Abraham, J. K.; Varadan, V. K. *Polym. Bull.* **2005**, *53*, 127.
(14) Xiong, S.; Xiao, Y.; Ma, J.; Zhang, L.; Lu, X. *Macromol. Rapid Commun.* **2007**, *28*, 281.
(15) Hirsch, A. *Angew Chem., Int. Ed.* **2002**, *41*, 1853.
(16) Neelgund, G. M.; Hrehorova, E.; Joyce, M.; Bliznyuk, V. *Polym. Int.* **2008**, *57*, 1083.
(17) Wu, M.; Snook, G. A.; Gupta, V.; Shaffer, M.; Fray, D. J.; Chen, G. Z. *J. Mater. Chem.* **2005**, *15*, 2297.
(18) (a) Wang, J.; Dai, J.; Yarlagadda, T. *Langmuir* **2005**, *21*, 9. (b) Xiong, S.; Phua, S. L.; Dunn, B. S.; Ma, J.; Lu, X. *Chem. Mater.* **2010**, *22*, 255.
(19) (a) Moon, H.; Park, J. *Solid State Ionics* **1999**, *120*, 1. (b) Ferloni, P.; Mastragostino, M.; Meneghello, L. *Electrochim. Acta* **1996**, *41*, 27.
(20) Pelster, R.; Nimtz, G.; Wessling, B. *Phys. Rev. B* **1994**, *49*, 12718.